MISCELLANEOUS PAPER GL-82-6

FREQUENCY RESPONSE CHARACTERISTICS OF MILITARY VEHICLES

by

Richard A. Weiss

Geotechnical Laboratory
U. S. Army Engineer Waterways Experiment Station
P. O. Box 631, Vicksburg, Miss. 39180

April 1982

Final Report

Approved For Public Release; Distribution Unlimited

Prepared for Assistant Secretary of the Army (R&D)
Department of the Army
Washington, D. C. 20310

Under Project No. 4A161101A91D

Unclassified
SECURITY CLASSIFICATION OF THIS PAGE *(When Data Entered)*

REPORT DOCUMENTATION PAGE

READ INSTRUCTIONS BEFORE COMPLETING FORM

1. REPORT NUMBER: Miscellaneous Paper GL-82-6
2. GOVT ACCESSION NO.:
3. RECIPIENT'S CATALOG NUMBER:

4. TITLE *(and Subtitle)*: FREQUENCY RESPONSE CHARACTERISTICS OF MILITARY VEHICLES

5. TYPE OF REPORT & PERIOD COVERED: Final report

6. PERFORMING ORG. REPORT NUMBER:

7. AUTHOR(s): Richard A. Weiss

8. CONTRACT OR GRANT NUMBER(s):

9. PERFORMING ORGANIZATION NAME AND ADDRESS:
U. S. Army Engineer Waterways Experiment Station
Geotechnical Laboratory
P. O. Box 631, Vicksburg, Miss. 39180

10. PROGRAM ELEMENT, PROJECT, TASK AREA & WORK UNIT NUMBERS: Project No. 4A161101A91D

11. CONTROLLING OFFICE NAME AND ADDRESS:
Assistant Secretary of the Army (R&D)
Department of the Army
Washington, D. C. 20310

12. REPORT DATE: April 1982

13. NUMBER OF PAGES: 56

14. MONITORING AGENCY NAME & ADDRESS*(if different from Controlling Office)*:

15. SECURITY CLASS. *(of this report)*: Unclassified

15a. DECLASSIFICATION/DOWNGRADING SCHEDULE:

16. DISTRIBUTION STATEMENT *(of this Report)*:
Approved for public release; distribution unlimited.

17. DISTRIBUTION STATEMENT *(of the abstract entered in Block 20, if different from Report)*:

18. SUPPLEMENTARY NOTES:
Available from National Technical Information Service, 5285 Port Royal Road, Springfield, Va. 22151.

19. KEY WORDS *(Continue on reverse side if necessary and identify by block number)*:
Frequency response (Dynamics)
Numerical analysis
Obstacles (Military science)
Vehicles, Military

20. ABSTRACT *(Continue on reverse side if necessary and identify by block number)*:

Empirical frequency response characteristics are calculated from the dynamic response data obtained from vehicles that are crossing obstacles. The frequency response signature for a vehicle is essentially the ratio of the power spectrum of the dynamic response of a vehicle to the power spectrum of the terrain feature producing the response. This study determines the acceleration frequency response signatures by calculating the Fourier series representation

(Continued)

DD FORM 1 JAN 73 1473 EDITION OF 1 NOV 65 IS OBSOLETE

Unclassified
SECURITY CLASSIFICATION OF THIS PAGE *(When Data Entered)*

20. ABSTRACT (Continued).

of the acceleration measured at a point on the vehicle as it crosses an obstacle and the Fourier series representation of the obstacle profile. The Fourier series representation of the measured acceleration is obtained by the fast Fourier transform algorithm. A numerical analysis was done for the M114 track vehicle. The empirical frequency response signature obtained for a vehicle from an obstacle crossing test can be used to predict the dynamic response of that vehicle for any other obstacle or terrain feature.

PREFACE

This study was conducted during the period October 1980 to December 1981 by personnel of the Geotechnical Laboratory (GL), U. S. Army Engineer Waterways Experiment Station (WES) for the Department of the Army Project No. 4A161101A91D, In-House Laboratory Independent Research (ILIR) Program, sponsored by the Assistant Secretary of the Army (R&D).

The study was conducted under the general supervision of Drs. W. F. Marcuson III and P. F. Hadala, Chief and Assistant Chief, respectively, of GL, and Messrs. C. J. Nuttall, Jr., Chief of the Mobility Systems Division (MSD), and D. D. Randolph, Chief of the Methodology and Modelling Group. Significant contributions were made by Mr. N. R. Murphy, Jr., of the Research Group. The report was written by Dr. R. A. Weiss, MSD.

COL Nelson P. Conover, CE, and COL Tilford C. Creel, CE, were Commanders and Directors of the WES during the conduct of this study and the preparation of this report. The Technical Director was Mr. Fred R. Brown.

CONTENTS

CONVERSION FACTORS, U. S. CUSTOMARY TO METRIC (SI)
UNITS OF MEASUREMENT

U. S. customary units of measurement used in this report can be converted to metric (SI) units as follows:

Multiply	By	To Obtain
cubic inches	16.38706	cubic centimetres
inches	25.4	millimetres
inches per second	25.4	millimetres per second
miles per hour (U. S. statute)	1.609344	kilometres per hour
square inches	6.4516	square centimetres
square inches per second	6.4516	square centimetres per second

FREQUENCY RESPONSE CHARACTERISTICS OF MILITARY VEHICLES

PART I: INTRODUCTION

Background

1. Driver safety standards and the design specifications of new electronic and optical equipment for vehicles require estimates of the values of the acceleration components expected to occur at a point on a vehicle when it crosses an obstacle or other terrain feature at a given speed. The electronic and optical equipment have shock and vibration criteria that are expressed by maximum acceleration tolerances. The driver tolerance is generally expressed as a limit on the power absorbed which in turn can be related to acceleration.[1,2] These criteria limit the speed at which a vehicle can cross obstacles and other terrain features.

2. A dynamical model of a vehicle is generally required to predict the acceleration components at a point on a vehicle as it runs over a specified terrain. This model consists of a combination of spring-mass-damper elements that are assembled to approximate as closely as possible the measured dynamic response of wheel and track laying vehicles. Many models of this type have been developed and used with varying degrees of success.[3,4] Within the limits of this formalism the predicted dynamic response of a vehicle will always be model dependent. In order to represent as closely as possible the actual interaction of a vehicle with terrain features it is of value to develop a model independent method for predicting the dynamical response of vehicles. Such a method can be developed to predict the root mean square (RMS) values of the acceleration components at a point on the vehicle.

3. It is possible to represent the RMS acceleration of a point on a vehicle as an integral of the acceleration power spectrum over all frequencies.[5-7] The power spectrum of a time dependent or space dependent quantity gives the amount of power associated with each constituent temporal or spatial frequency component of the Fourier representation of

the physical quantity.[8,9] The time history of the acceleration of a point on a vehicle has a corresponding acceleration power spectrum which depends on the temporal frequencies, while the spatial variations of terrain features has an associated power spectrum which depends on the spatial frequencies. The frequency response signature for the acceleration components of a vehicle is the ratio of the acceleration power spectrum to the power spectrum of the terrain elevation variations. All of the dynamical characteristics of a vehicle are contained in its frequency response signatures, so that if these signatures are obtained empirically they can serve as a model independent representation of the dynamical response of a vehicle.

Objectives

4. The basic objective of this report is the development of a semiempirical, model independent, method of predicting the dynamical response of a vehicle as it crosses an obstacle or other terrain feature. The specific objectives of this study are (Figure 1):

   a. The employment of Fourier analysis to describe the frequency content of various obstacle profiles and the frequency content of the measured dynamic response of a vehicle.

   b. The development of a method for determining the frequency response signatures of a vehicle from the acceleration time histories measured at a point on a vehicle as it crosses an obstacle of known profile.

Scope

5. The following specific work was done (Figure 2):

   a. A catalog of Fourier transforms was developed for several basic obstacle shapes.

   b. The fast Fourier transform (FFT) was used to determine the Fourier spectrum of the acceleration time history measured at a point on a vehicle as it crosses an obstacle of known profile.

   c. Dimensionless acceleration frequency response signatures

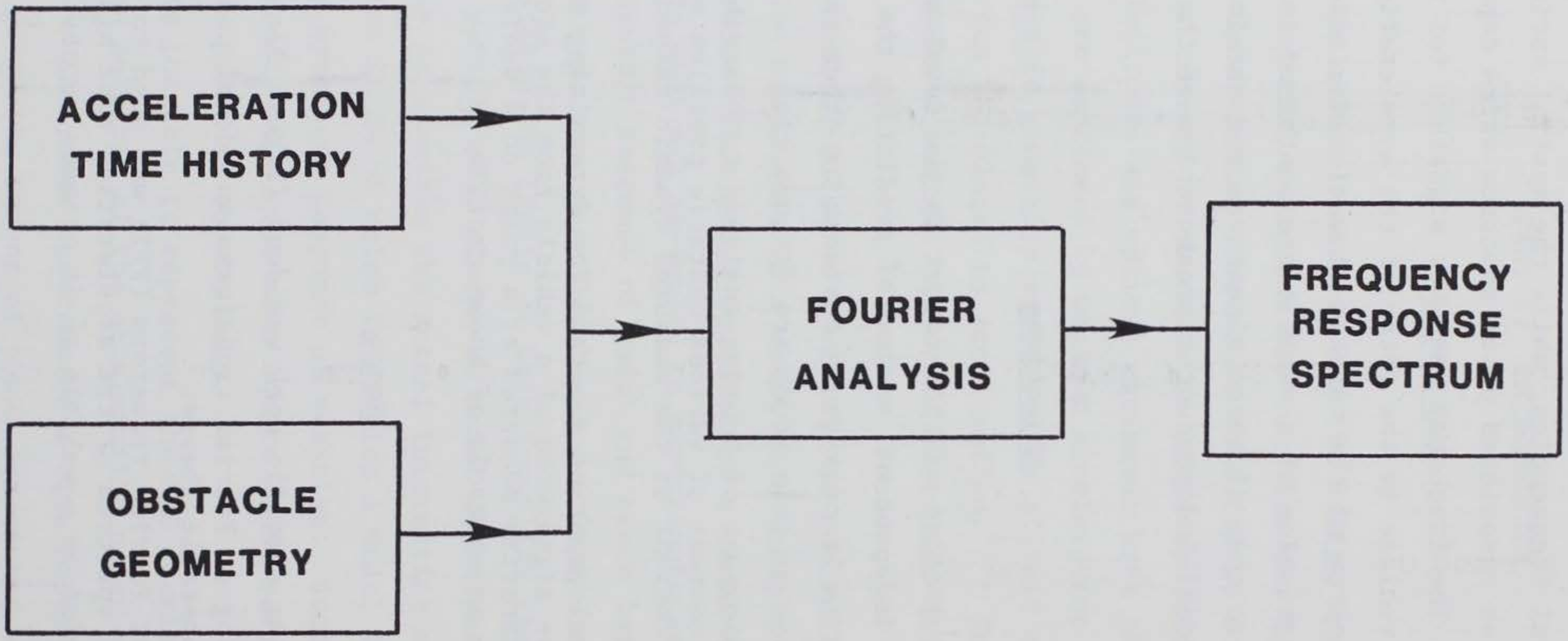

Figure 1. Objectives

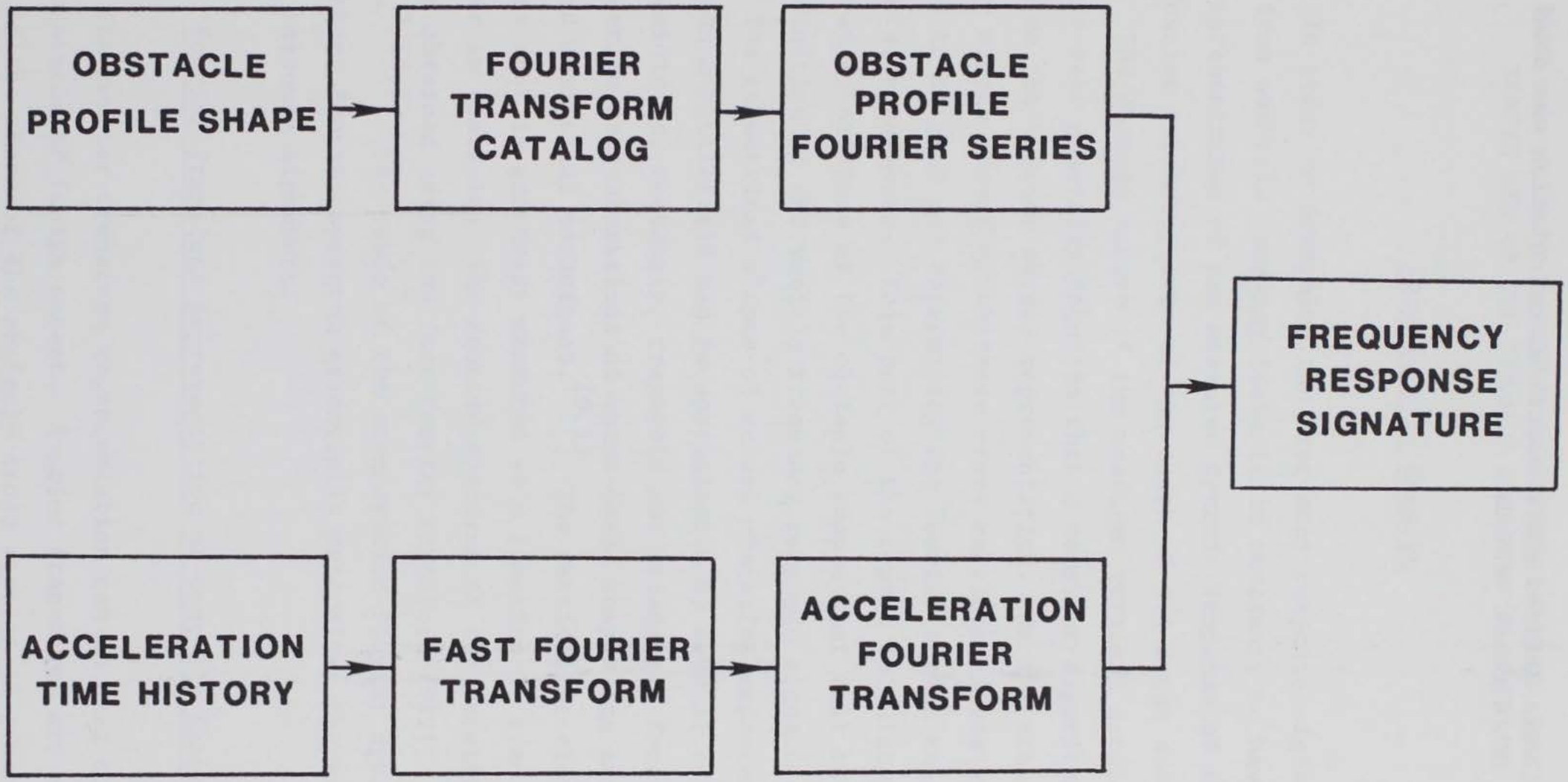

Figure 2. Scope

were defined and a numerical calculation was done for an M114 track vehicle.

PART II: FOURIER SPECTRUM REPRESENTATIONS OF OBSTACLE SHAPES AND OF THE DYNAMIC RESPONSE OF VEHICLES

Introductory Remarks

6. In order to determine the frequency response signatures of vehicles from obstacle crossing tests it is necessary to have both the Fourier representation of the measured dynamic response of the vehicle and the Fourier representation of the shape of the cross section of the obstacle. The chaotic nature of the measured vertical acceleration at the drivers seat generally requires that a computer algorithm be used to determine the Fourier series representation. On the other hand the relatively simple shapes of obstacle cross sections allows analytical techniques to be used for determining the Fourier series representation of the obstacle geometry. This part of the report calculates the Fourier spectral representations of the obstacle shapes that will be used for the determination of the vehicle frequency response signatures.

7. The geometrical shapes of actual obstacles expected to be encountered on a battlefield can be approximated by several basic geometric shapes--semicircle, rectangle, trapezoid and triangle. Fourier transform and series representations of these basic shapes are easily obtained by standard analytical techniques.[10,11] The vertical acceleration at the drivers seat is generally measured as a function of time as a vehicle passes over an obstacle. The Fourier spectrum of the acceleration time history is obtained using the fast Fourier transform (FFT) algorithm.[7,12,13] The ratio of the acceleration Fourier spectrum to the obstacle shape Fourier spectrum essentially determines the vehicle's frequency response signature.

Fourier Transform Representation of Obstacle Shapes

8. The Fourier transform representation can be used to describe a single obstacle of finite extent. Fourier transforms are easier to calculate if the shape of the obstacle cross section is symmetrical about

a vertical axis. If the axis of evaluation of a symmetrical obstacle is taken to be the axis of symmetry the Fourier transform reduces to the Fourier cosine transform (Figure 3). If the axis of symmetry of a

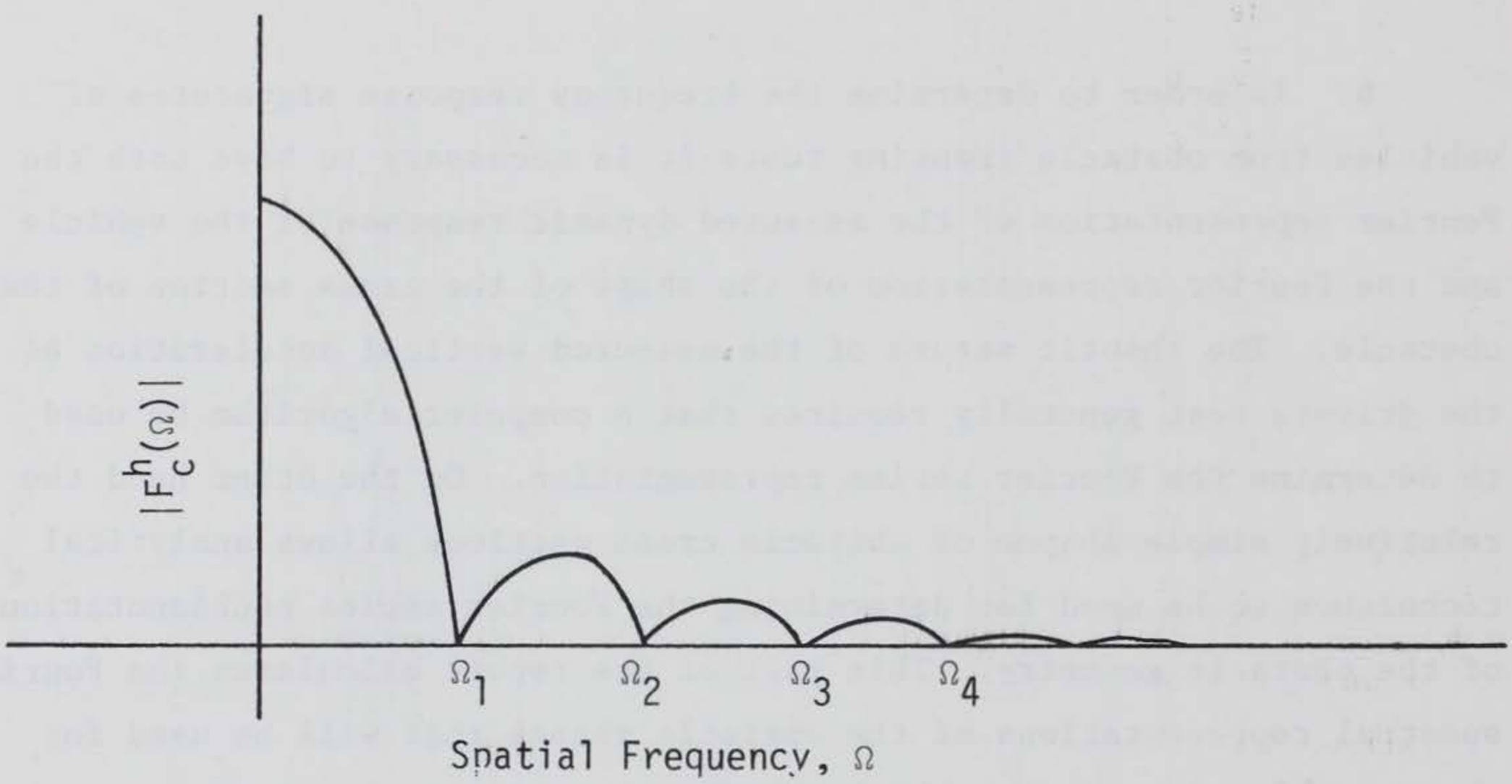

Figure 3. Typical Fourier cosine transform

symmetrical obstacle is not chosen as the axis of representation or if the obstacle is asymmetrical, both Fourier cosine and Fourier sine transforms are required. The Fourier cosine transform pairs are written as[10]

$$F_c^h(k) = \sqrt{\frac{2}{\pi}} \int_0^\infty h(\xi) \cos k\xi d\xi \qquad (1)$$

$$h(\xi) = \sqrt{\frac{2}{\pi}} \int_0^\infty F_c^h(k) \cos k\xi dk \qquad (2)$$

where

$h(\xi)$ = height of obstacle cross section

$F_c^h(k)$ = Fourier cosine transform of obstacle shape

k = wave number = $2\pi/\lambda$ where λ = spatial wavelength components

Defining the spatial frequency as $\Omega = 1/\lambda$ yields the following relation $k = 2\pi\Omega$.

9. For the case of an asymmetrical obstacle shape the following complex Fourier transform is used[10]

$$\tilde{I}^h(k) = \frac{1}{\sqrt{2\pi}} \int_{-\infty}^{\infty} h(x) e^{ikx} dx \tag{3}$$

$$= I_c^h(k) + iI_s^h(k) = I^h(k) e^{i\phi^h(k)}$$

$$h(x) = \frac{1}{\sqrt{2\pi}} \int_{-\infty}^{\infty} \tilde{I}^h(k) e^{-ikx} dk \tag{4}$$

$$= \sqrt{\frac{2}{\pi}} \int_{o}^{\infty} I^h(k) \cos (kx - \phi^h) dk$$

where

$$I_c^h(k) = \frac{1}{\sqrt{2\pi}} \int_{-\infty}^{\infty} h(x) \cos kx dx \tag{5}$$

$$I_s^h(k) = \frac{1}{\sqrt{2\pi}} \int_{-\infty}^{\infty} h(x) \sin kx dx \tag{6}$$

$$I^h(k) = \sqrt{\left(I_c^h\right)^2 + \left(I_s^h\right)^2} \tag{7}$$

$$\phi^h(k) = \tan^{-1}\left[\frac{I_s^h(k)}{I_c^h(k)}\right] \tag{8}$$

and where

$\tilde{I}^h(k)$ = complex Fourier transform

$I_c^h(k)$ = real part of $\tilde{I}^h(k)$

$I_s^h(k)$ = imaginary part of $\tilde{I}^h(k)$

$I^h(k)$ = magnitude of $\tilde{I}^h(k)$

$\phi^h(k)$ = phase angle of the complex Fourier transform $\tilde{I}^h(k)$

10. For the special case of a symmetrical obstacle of length $2L_o$, with the origin of the axis chosen at the left edge of the obstacle and the symmetry axis at L_o, the Fourier transform components are given in Appendix A

$$I_c^h(k) = F_c^h(k) \cos kL_o \tag{9}$$

$$I_s^h(k) = F_c^h(k) \sin kL_o \tag{10}$$

$$I^h(k) = \left|F_c^h(k)\right| \tag{11}$$

$$\phi^h(k) = kL_o + n\pi \tag{12}$$

For a symmetrical obstacle with the origin of the axis chosen to be at the axis of symmetry the Fourier transform is obtained as

$$I_c^h(k) = F_c^h(k) \tag{13}$$

$$I_s^h(k) = 0 \tag{14}$$

$$I^h(k) = \left| F_c^h(k) \right| \tag{15}$$

$$\phi^h(k) = n\pi \tag{16}$$

which is just the Fourier cosine transform.

11. The dynamical response (acceleration) of several military vehicles encountering obstacles has been measured for basic obstacle shapes including the semicircle, rectangle and trapezoid. Therefore the Fourier transforms of several basic symmetrical and asymmetrical obstacles have been evaluated in Appendix A and are tabulated below:

Semicircle (Figure 4a)

$$F_c^h(k) = \sqrt{\frac{2}{\pi}} \left(\frac{\pi R^2}{4}\right)\left[\frac{2J_1(kR)}{kR}\right]$$

$$I_c^h(k) = F_c^h(k) \cos kR$$

$$I_s^h(k) = F_c^h(k) \sin kR$$

$$I^h(k) = \left| F_c^h(k) \right|$$

Rectangle (Figure 4b)

$$F_c^h(k) = \sqrt{\frac{2}{\pi}}\, ah\left(\frac{\sin ka}{ka}\right)$$

$$I_c^h(k) = F_c^h(k) \cos ka$$

$$I_s^h(k) = F_c^h(k) \sin ka$$

$$I^h(k) = \left| F_c^h(k) \right|$$

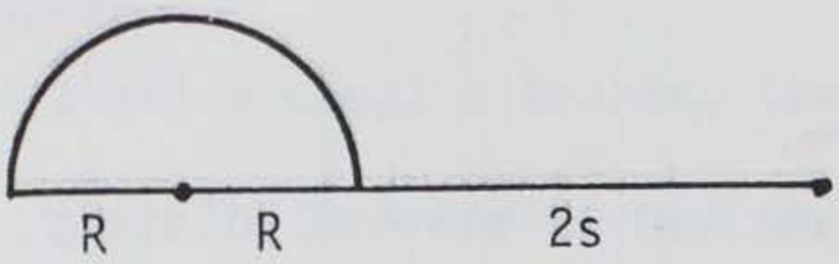

$2L_o = 2R$

$2L = 2(R + s)$

a. Semicircle

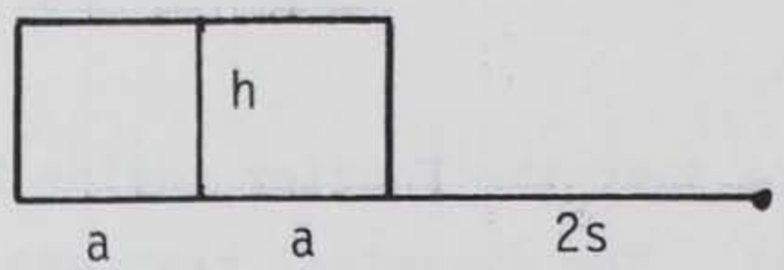

$2L_o = 2a$

$2L = 2a + 2s$

b. Rectangle

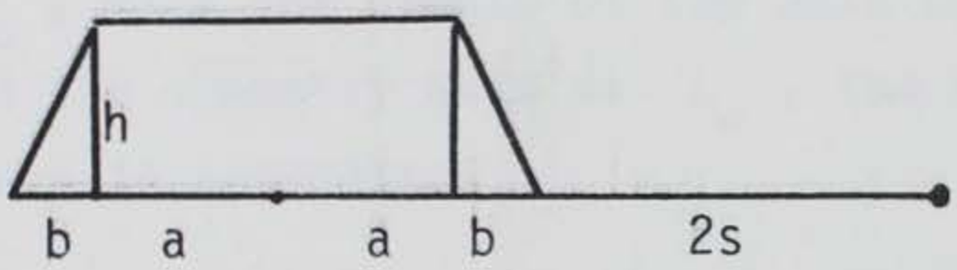

$2L_o = 2(a + b)$

$2L = 2(a + b + s)$

c. Symmetrical trapezoid

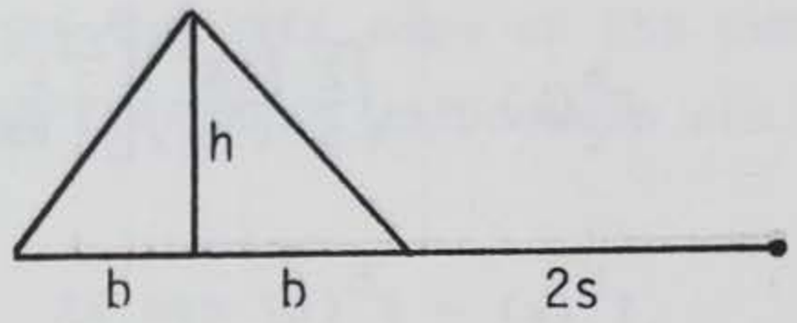

$2L_o = 2b$

$2L = 2(b + s)$

d. Symmetrical triangle

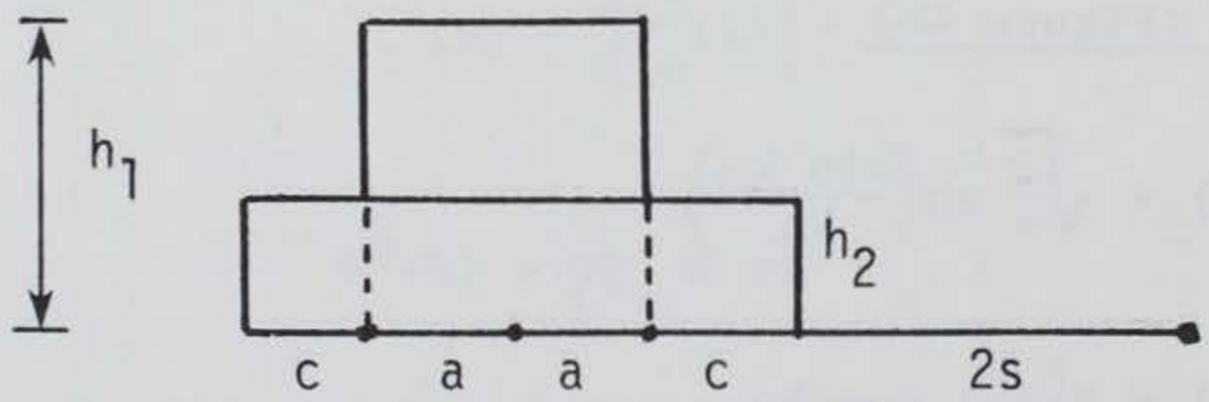

$2L_o = 2(a + c)$

$2L = 2(a + c + s)$

e. Double rectangle

Figure 4. Symmetrical obstacle shapes

Symmetrical trapezoid (Figure 4c)

$$F_c^h(k) = \sqrt{\frac{2}{\pi}}\left(a + \frac{b}{2}\right)h\left[\frac{\sin k(a + b/2)}{k(a + b/2)}\right]\left(\frac{\sin kb/2}{kb/2}\right)$$

$$I_c^h(k) = F_c^h(k) \cos k(a + b)$$

$$I_s^h(k) = F_c^h(k) \sin k(a + b)$$

$$I^h(k) = \left|F_c^h(k)\right|$$

Symmetrical triangle (Figure 4d)

$$F_c^h(k) = \sqrt{\frac{2}{\pi}}\left(\frac{bh}{2}\right)\left(\frac{\sin bk/2}{kb/2}\right)^2$$

$$I_c^h(k) = F_c^h(k) \cos kb$$

$$I_s^h(k) = F_c^h(k) \sin kb$$

$$I^h(k) = \left|F_c^h(k)\right|$$

Double rectangle (Figure 4e)

$$F_c^h(k) = \sqrt{\frac{2}{\pi}}\left[h_1 a\left(\frac{\sin ka}{ka}\right) + h_2 c\left(\frac{\sin kc/2}{kc/2}\right)\cos k(a + c/2)\right]$$

$$I_c^h(k) = F_c^h(k) \cos k(a + c)$$

$$I_s^h(k) = F_c^h(k) \sin k(a + c)$$

$$I^h(k) = \left|F_c^h(k)\right|$$

Asymmetrical trapezoid (Figure 5a)

$$I_c^h(o) = \frac{h}{\sqrt{2\pi}}\left[2a + \frac{(b + e)}{2}\right]$$

$$I_c^h(k) = \frac{1}{\sqrt{2\pi}} \frac{h}{k}\left[\sin k\left(2a + b + \frac{e}{2}\right)\frac{\sin ke/2}{ke/2} - \frac{kb}{2}\left(\frac{\sin kb/2}{kb/2}\right)^2\right] .$$

$$I_s^h(k) = \frac{1}{\sqrt{2\pi}} \frac{h}{k}\left[\frac{\sin kb}{kb} - \left(\frac{\sin ke/2}{ke/2}\right) \cos k\left(2a + b + \frac{e}{2}\right)\right]$$

$$I^h(k) = \frac{1}{\sqrt{2\pi}} \frac{h}{k} \sqrt{\left(\frac{\sin kb/2}{kb/2}\right)^2 + \left(\frac{\sin ke/2}{ke/2}\right)^2 - 2\left(\frac{\sin kb/2}{kb/2}\right)\left(\frac{\sin ke/2}{ke/2}\right) \cos k\left[2a + \frac{(b + e)}{2}\right]}$$

$$\phi^h(o) = 0$$

$$\phi^h(k) = \tan^{-1}\left[\frac{I_s^h(k)}{I_c^h(k)}\right]$$

Right angle trapezoid (Figure 5b)

$$I_c^h(o) = \frac{h}{\sqrt{2\pi}}\left(2a + \frac{b}{2}\right)$$

$$I_c^h(k) = \frac{1}{\sqrt{2\pi}} \frac{h}{k}\left[\sin k(2a + b) - \frac{kb}{2}\left(\frac{\sin kb/2}{kb/2}\right)^2\right]$$

$$I_s^h(k) = \frac{1}{\sqrt{2\pi}} \frac{h}{k}\left[\frac{\sin kb}{kb} - \cos k(2a + b)\right]$$

$$I^h(k) = \frac{1}{\sqrt{2\pi}} \frac{h}{k} \sqrt{1 + \left(\frac{\sin kb/2}{kb/2}\right)^2 - 2\left(\frac{\sin kb/2}{kb/2}\right) \cos k(2a + b/2)}$$

$$\phi^h(k) = \tan^{-1}\left[\frac{I_s^h(k)}{I_c^h(k)}\right]$$

$$\phi^h(o) = 0$$

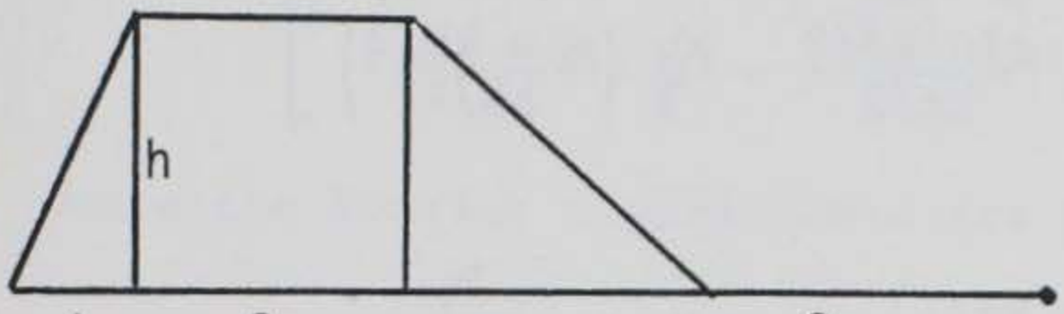

$2L_o = b + e + 2a$

$2L = b + e + 2(a + s)$

a. Asymmetrical trapezoid

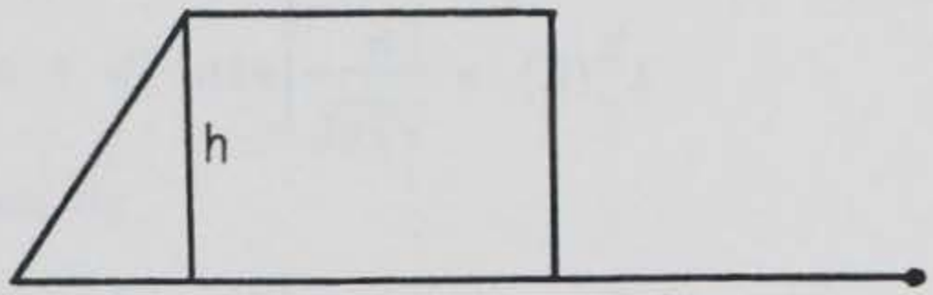

$2L_o = b + 2a$

$2L = b + 2(a + s)$

b. Right angle trapezoid

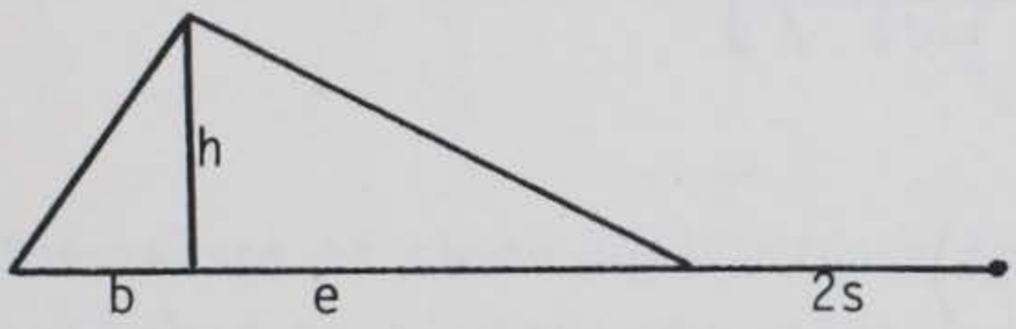

$2L_o = b + e$

$2L = b + e + 2s$

c. Asymmetrical triangle

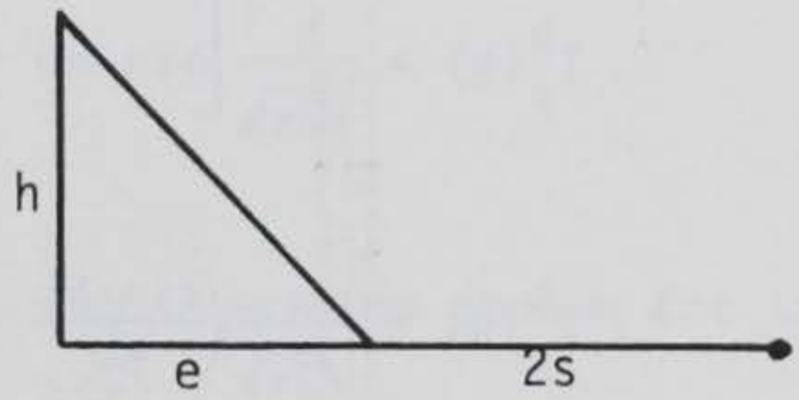

$2L_o = e$

$2L = e + 2s$

d. Right triangle

Figure 5. Asymmetrical obstacle shapes

Asymmetrical triangle (Figure 5c)

$$I_c^h(o) = \frac{h}{\sqrt{2\pi}} \frac{(b + e)}{2}$$

$$I_c^h(k) = \frac{h}{\sqrt{2\pi}k}\left[\sin\ (b + e/2)\ \frac{\sin\ ke/2}{ke/2} - \frac{kb}{2}\left(\frac{\sin\ kb/2}{kb/2}\right)^2\right]$$

$$I_s^h(k) = \frac{h}{\sqrt{2\pi}k}\left[\frac{\sin\ kb}{kb} - \left(\frac{\sin\ ke/2}{ke/2}\right)\cos\ k(b + e/2)\right]$$

$$I^h = \frac{h}{\sqrt{2\pi}k}\sqrt{\left(\frac{\sin\ kb/2}{kb/2}\right)^2 + \left(\frac{\sin\ ke/2}{ke/2}\right)^2 - 2\left(\frac{\sin\ kb/2}{kb/2}\right)\left(\frac{\sin\ ke/2}{ke/2}\right)\cos\ k\left(\frac{b + e}{2}\right)}$$

Right triangle (Figure 5d)

$$I_c^h(o) = \frac{h}{\sqrt{2\pi}} \frac{b}{2}$$

$$I_c^h(k) = \frac{h}{\sqrt{2\pi}k}\left[\sin\ kb - \frac{kb}{2}\left(\frac{\sin\ kb/2}{kb/2}\right)^2\right]$$

$$I_s^h(k) = \frac{h}{\sqrt{2\pi}k}\left(\frac{\sin\ kb}{kb} - \cos\ kb\right)$$

$$I^h(k) = \frac{h}{\sqrt{2\pi}k}\left[1 + \left(\frac{\sin\ kb/2}{kb/2}\right)^2 - 2\left(\frac{\sin\ kb/2}{kb/2}\right)\cos\ \frac{kb}{2}\right]$$

Fourier Series Representation of Obstacle Shapes

12. A Fourier series representation of an obstacle cross section can be obtained from the calculated Fourier transform. Fourier series are defined only for periodic functions and therefore to obtain a Fourier series representation of an obstacle shape, the cross section must be taken to be one of an infinite set of obstacles which repeat in a period $2L$. The period $2L$ can be selected arbitrarily except that it must be

taken larger than the width of the obstacle cross section (Figures 4 and 5). The Fourier series can then be written as[11]

$$h(x) = \frac{A_o^h}{2} + \sum_{n=1}^{\infty} \left(A_n^h \cos k_n x + B_n^h \sin k_n x \right) \tag{17}$$

where the Fourier coefficients are given by

$$A_n^h = \frac{1}{L} \int_{-L}^{L} h(x) \cos k_n x dx \qquad n = 0, 1, 2, 3, \ldots \tag{18}$$

$$B_n^h = \frac{1}{L} \int_{-L}^{L} h(x) \sin k_n x dx \qquad n = 1, 2, 3, \ldots \tag{19}$$

and where the wave number k_n is given by

$$k_n = \frac{n\pi}{L} \; . \tag{20}$$

The values of these coefficients depend on the position chosen for the axis used to describe the shape function $h(x)$.

13. The Fourier series can also be written in the following form

$$h(x) = \frac{A_o^h}{2} + \sum_{n=1}^{\infty} C_n^h \cos \left(\frac{n\pi x}{L} - \phi_n^h \right) \tag{21}$$

where

$$C_n^h = \sqrt{\left(A_n^h\right)^2 + \left(B_n^h\right)^2} \tag{22}$$

$$A_n^h = C_n^h \cos \phi_n^h \tag{23}$$

$$B_n^h = C_n^h \sin \phi_n^h \tag{24}$$

$$\phi_n^h = \tan^{-1}\left(\frac{B_n^h}{A_n^h}\right) \tag{25}$$

For the special case of a symmetrical obstacle cross section with the axis for the representation of $h(x)$ chosen to be the axis of symmetry, the Fourier cosine series can be used as follows[11]

$$h(x) = \frac{a_o^h}{2} + \sum_{n=1}^{\infty} a_n^h \cos \frac{n\pi x}{L} \tag{26}$$

where

$$a_n^h = \frac{2}{L}\int_o^L h(x) \cos \frac{n\pi x}{L}\, dx \tag{27}$$

for $n = 0, 1, 2, 3, \ldots$.

14. For a symmetrical obstacle of length $2L_o$ with the coordinate axis chosen at the left hand edge of $h(x)$, the Fourier series coefficients are obtained from Equations 18, 19, and 27 to be

$$A_n^h = a_n^h \cos k_n L_o \tag{28}$$

$$B_n^h = a_n^h \sin k_n L_o \tag{29}$$

$$C_n^h = \left|a_n^h\right| \tag{30}$$

$$\phi_n^h = k_n L_o \tag{31}$$

where a_n^h is given by Equation 27. For the case of a symmetrical obstacle with the axis of representation of $h(x)$ taken to be the axis of symmetry, the Fourier coefficients are given by

$$A_n^h = a_n^h \tag{32}$$

$$B_n^h = 0 \tag{33}$$

$$C_n^h = \left| a_n^h \right| \tag{34}$$

$$\phi_n^h = 0 \tag{35}$$

which is the Fourier cosine series of Equations 26 and 27.

15. A simple relationship exists between the Fourier transform functions and the Fourier series coefficients for obstacles of period $2L$. The Fourier series coefficients can be obtained by making the replacements $\sqrt{2\pi} \to L$ and $k \to k_n$. With these replacements it follows from Equations 1-27 that[10]:

$$a_n^h = \frac{\sqrt{2\pi}}{L} F_c^h(k_n) \tag{36}$$

$$A_n^h = \frac{\sqrt{2\pi}}{L} I_c^h(k_n) \tag{37}$$

$$B_n^h = \frac{\sqrt{2\pi}}{L} I_s^h(k_n) \tag{38}$$

$$C_n^h = \frac{\sqrt{2\pi}}{L} I^h(k_n) \tag{39}$$

$$\phi_n^h = \tan^{-1}\left(\frac{I_s^h(k_n)}{I_c^h(k_n)}\right) \tag{40}$$

Fourier Spectrum Representation of the Dynamic Response of a Vehicle

16. A frequently measured quantity in vehicle ride quality studies is the time history of the vertical acceleration produced at the driver's seat when the vehicle encounters an obstacle. This dynamic response is generally irregular and chaotic, and numerical methods must be used for a Fourier analyses. The FFT algorithm is well suited for obtaining the Fourier series coefficients for the measured acceleration time history. The corresponding Fourier transforms can then be calculated in terms of the Fourier series coefficients. The Fourier transforms and Fourier series of the dynamic response will now be written out explicitly because these quantities appear in the definition of the frequency response signatures that are calculated in Part III.

17. The Fourier transform pairs that describe the acceleration, velocity, and displacement at the driver's seat can be written as

$$a(t) = \frac{1}{\sqrt{2\pi}} \int_{-\infty}^{\infty} \tilde{I}^a(\omega) e^{-i\omega t} d\omega \tag{41}$$

$$v(t) = \frac{1}{\sqrt{2\pi}} \int_{-\infty}^{\infty} \tilde{I}^v(\omega) e^{-i\omega t} d\omega \tag{42}$$

$$d(t) = \frac{1}{\sqrt{2\pi}} \int_{-\infty}^{\infty} \tilde{I}^d(\omega) e^{-i\omega t} d\omega \tag{43}$$

where

a(t) = time history of the vertical acceleration

v(t) = time history of the velocity

d(t) = time history of the displacement

The Fourier transforms are then written as

$$\tilde{I}^{a}(\omega) = \frac{1}{\sqrt{2\pi}} \int_{-\infty}^{\infty} a(t) e^{i\omega t} dt \tag{44}$$

$$\tilde{I}^{v}(\omega) = \frac{1}{\sqrt{2\pi}} \int_{-\infty}^{\infty} v(t) e^{i\omega t} dt \tag{45}$$

$$\tilde{I}^{d}(\omega) = \frac{1}{\sqrt{2\pi}} \int_{-\infty}^{\infty} d(t) e^{i\omega t} dt \tag{46}$$

where

$\tilde{I}^{a}(\omega)$ = complex Fourier transform of the acceleration at the driver's seat

$\tilde{I}^{v}(\omega)$ = complex Fourier transform of the velocity at the driver's seat

$\tilde{I}^{d}(\omega)$ = complex Fourier transform of the displacement at the driver's seat

$\omega = 2\pi f$ = angular frequency

18. The complex Fourier transforms can be written as[10,11]

$$\tilde{I}^{a}(\omega) = I_c^a(\omega) + iI_s^a(\omega) = I^a(\omega) e^{i\phi^a(\omega)} \tag{47}$$

$$\tilde{I}^{v}(\omega) = I_c^v(\omega) + iI_s^v(\omega) = I^v(\omega) e^{i\phi^v(\omega)} \tag{48}$$

$$\tilde{I}^{d}(\omega) = I_c^d(\omega) + iI_s^d(\omega) = I^d(\omega) e^{i\phi^d(\omega)} \tag{49}$$

where

$$I_c^a(\omega) = \frac{1}{\sqrt{2\pi}} \int_{-\infty}^{\infty} a(t) \cos \omega t dt \tag{50}$$

$$I_s^a(\omega) = \frac{1}{\sqrt{2\pi}} \int_{-\infty}^{\infty} a(t) \sin \omega t dt \tag{51}$$

$$I^a(\omega) = \sqrt{\left(I_c^a\right)^2 + \left(I_s^a\right)^2} \tag{52}$$

$$\phi^a(\omega) = \tan^{-1}\left(\frac{I_s^a}{I_c^a}\right) \tag{53}$$

$$I_c^v(\omega) = \frac{1}{\sqrt{2\pi}} \int_{-\infty}^{\infty} v(t) \cos \omega t dt \tag{54}$$

$$I_s^v(\omega) = \frac{1}{\sqrt{2\pi}} \int_{-\infty}^{\infty} v(t) \sin \omega t dt \tag{55}$$

$$I^v(\omega) = \sqrt{\left(I_c^v\right)^2 + \left(I_s^v\right)^2} \tag{56}$$

$$\phi^v(\omega) = \tan^{-1}\left(\frac{I_s^v}{I_c^v}\right) \tag{57}$$

$$I_c^d(\omega) = \frac{1}{\sqrt{2\pi}} \int_{-\infty}^{\infty} d(t) \cos \omega t dt \tag{58}$$

$$I_s^d(\omega) = \frac{1}{\sqrt{2\pi}} \int_{-\infty}^{\infty} d(t) \sin \omega t dt \tag{59}$$

$$I^d(\omega) = \sqrt{\left(I_c^d\right)^2 + \left(I_s^d\right)^2} \tag{60}$$

$$\phi^d(\omega) = \tan^{-1}\left(\frac{I_s^d}{I_c^d}\right) \tag{61}$$

19. The corresponding Fourier series representations of the time histories of the dynamical response at the driver's seat are written as

$$a(t) = \frac{A_o^a}{2} + \sum_{n=1}^{\infty} \left(A_n^a \cos \omega_n t + B_n^a \sin \omega_n t\right) \tag{62}$$

$$= \sum_{n=0}^{\infty} C_n^a \cos (\omega_n t - \phi_n^a)$$

$$v(t) = \frac{A_o^v}{2} + \sum_{n=1}^{\infty} (A_n^v \cos \omega_n t + B_n^v \sin \omega_n t) \tag{63}$$

$$= \sum_{n=0}^{\infty} C_n^v \cos (\omega_n t - \phi_n^v)$$

$$d(t) = \frac{A_o^d}{2} + \sum_{n=1}^{\infty} \left(A_n^d \cos \omega_n t + B_n^d \sin \omega_n t \right) \tag{64}$$

$$= \sum_{n=0}^{\infty} C_n^d \cos \left(\omega_n t - \phi_n^d \right)$$

where

$\omega_n = n\pi/T$

$2T$ = period chosen to represent the time history

The relationship between the Fourier series representation and the Fourier transform representation of the dynamic response of the vehicle is given by

$$A_n^{a,v,d} = \frac{\sqrt{2\pi}}{T} I_c^{a,v,d}(\omega_n) \tag{65}$$

$$B_n^{a,v,d} = \frac{\sqrt{2\pi}}{T} I_s^{a,v,d}(\omega_n) \tag{66}$$

$$C_n^{a,v,d} = \frac{\sqrt{2\pi}}{T} I^{a,v,d}(\omega_n) \tag{67}$$

$$\phi_n^{a,v,d} = \phi^{a,v,d}(\omega_n) \tag{68}$$

Either Fourier representation can be obtained from the other, so that the representation easiest to obtain from the measured data can always be used to determine the alternate representation.

20. Generally only the time history of the acceleration at the drivers seat is measured, but the velocity and displacement time histories can be obtained by numerical integration with proper choice of initial conditions. The measured acceleration time history is generally very complicated and chaotic, and an accurate determination of the

Fourier transforms by direct integration is expensive and time consuming. Therefore an alternative method for calculating the Fourier transforms or series is required. A rapid and inexpensive method of calculating the Fourier series coefficients is given by the fast Fourier transform (FFT).

21. The FFT is a mathematical procedure for rapidly determining the Fourier series of a specified function.[12,13] The algorithm requires 2^n pairs of data points t_j, $a(t_j)$ from which half that number of Fourier coefficient pairs A_j^a, B_j^a are determined. The accuracy of the calculated Fourier series coefficients improves as the number of data points describing the function increases. The Fourier transforms can then be estimated in terms of the Fourier series coefficients by using Equations 65-68.

22. The vehicle frequency signature that is calculated in Part III is essentially a comparison (ratio) of the Fourier representation of a vehicle response to the Fourier representation of an obstacle shape. These Fourier representations must be compatible in the sense that both must be either Fourier transforms or Fourier series. Also, the half-period L of the Fourier series representation of an obstacle shape must be related to the half-period T of the Fourier series representation of an acceleration time history by the equation $L = uT$ where u = vehicle speed which is assumed to be constant. From Equations 39 and 67 it follows that

$$\frac{C_n^{a,v,d}}{C_n^h} = u \frac{I^{a,v,d}(\omega_n)}{I^h(k_n)} \tag{69}$$

Equation 69 is basic to the calculation of the frequency response signatures done in Part III.

PART III: VEHICLE FREQUENCY RESPONSE SIGNATURES

Introductory Remarks

23. The frequency response signature of a vehicle, which will be defined and calculated here, is essentially the ratio of the power spectrum of the acceleration response of a vehicle to the power spectrum of the terrain feature producing the acceleration response. The acceleration response of a vehicle generally has three components that are associated with the heaving, pitching, and rolling motion of the vehicle, so that three distinct frequency spectrum signatures are required for a complete description of each vehicle. Knowledge of the frequency response signatures makes possible the prediction of the vehicle response to any terrain features.

24. Model dependent expressions for the frequency response signatures have already appeared in the literature, and in principle these signatures are vehicle characteristics that depend on the dynamical response parameters of a vehicle and on the geometry of the vehicle-ground contact area.[8,9] This part of the report gives a model independent method of determining the frequency response signatures from the acceleration time histories measured at a point on a vehicle as it crosses an obstacle of known shape.

Calculation of the Frequency Response Signatures

Definitions and terms

25. The vehicle frequency response signatures are dimensionless functions that relate the dynamic response of a vehicle to the terrain elevations that produce the response. The frequency content of the terrain elevation variations can be described by a frequency spectrum analysis using power spectra.[5,8,9] Obstacles can be handled in a similar fashion and have the advantage that their Fourier spectra are easily calculated. A simple relationship exists between the power spectrum and the Fourier amplitudes of elevation variations, so that the power spectra

associated with the Fourier spectra of Part II are easily calculated.

26. The power spectrum describes the frequency content of the variations of a physical quantity in such a way that the integral of the power spectrum over all frequencies is related to the root mean square (RMS) of the physical variable.[5,7,9,10] For instance, for a terrain elevation such as an obstacle

$$\Sigma_h^2 = \int_0^\infty P_h(\Omega)\,d\Omega = \int_0^\infty P_h(f)\,df \tag{70}$$

where

Σ_h = RMS of the obstacle profile

$P_h(\Omega)$ = power spectrum of the obstacle profile expressed in terms of the spatial frequency

$P_h(f)$ = power spectrum of the obstacle profile expressed in terms of the time frequency

and where the time frequency is related to the spatial frequency by

$$f = u\Omega \tag{71}$$

where u equals the horizontal speed of the vehicle which is assumed to be constant during transit of the obstacle. From Equations 70 and 71 it follows that

$$P_h(\Omega) = uP_h(f) \tag{72}$$

27. A complete description of the dynamic response of a vehicle includes the time histories of the acceleration, velocity, and displacement of a point on the vehicle during transit of the obstacle. In practice only the three components of the acceleration are measured. However, for completeness the frequency response signatures of the acceleration, velocity, and displacement will be considered. The frequency spectrum signatures relate the power spectra of the dynamic

response of the vehicle to the power spectrum of the obstacle profile and are defined as follows:

$$\Sigma_a^2 = \int_0^\infty P_a(f)df \equiv \int_0^\infty (2\pi f)^4 S_a(f)P_h(f)df \tag{73}$$

$$\Sigma_v^2 = \int_0^\infty P_v(f)df \equiv \int_0^\infty (2\pi f)^2 S_v(f)P_h(f)df \tag{74}$$

$$\Sigma_d^2 = \int_0^\infty P_d(f)df \equiv \int_0^\infty S_d(f)P_h(f)df \tag{75}$$

where

Σ_a = RMS of the acceleration of a point on the vehicle for one of the three modes of motion

Σ_v = RMS of the velocity of a point on the vehicle for one of the three possible modes of motion

Σ_d = RMS of the displacement of a point on the vehicle for one of the three possible modes of motion

$P_a(f)$ = power spectrum of the acceleration modes

$P_v(f)$ = power spectrum of the velocity modes

$P_d(f)$ = power spectrum of the displacement modes

$S_a(f)$ = acceleration frequency response signatures

$S_v(f)$ = velocity frequency response signatures

$S_d(f)$ = displacement frequency response signatures

Because the acceleration, velocity, and displacement each has three components, there are in principle nine frequency response signatures. In practice only the three acceleration frequency response signatures are measured.

Frequency response signatures for acceleration, velocity and displacement

28. From Equations 72-75 it follows that the frequency response signatures are given by

$$S_a(f) = \frac{P_a(f)}{(2\pi f)^4 P_h(f)} = \frac{uP_a(f)}{(2\pi f)^4 P_h(\Omega)} \tag{76}$$

$$S_v(f) = \frac{P_v(f)}{(2\pi f)^2 P_h(f)} = \frac{uP_v(f)}{(2\pi f)^2 P_h(\Omega)} \tag{77}$$

$$S_d(f) = \frac{P_d(f)}{P_h(f)} = \frac{uP_d(f)}{P_h(\Omega)} \tag{78}$$

For the purpose of numerical calculations it is necessary to express the power spectra in Equations 76-78 in terms of Fourier amplitudes which are obtained from a frequency spectrum analysis of the obstacle profile and the measured time histories of the dynamical vehicle response.

29. The power spectrum of a function is related to the square of the magnitude of the Fourier transform of the function as follows[7]

$$P_a(f) = f_o \left| I^a(\omega) \right|^2 \tag{79}$$

$$P_v(f) = f_o \left| I^v(\omega) \right|^2 \tag{80}$$

$$P_d(f) = f_o \left| I^d(\omega) \right|^2 \tag{81}$$

$$P_h(\Omega) = \Omega_o \left| I^h(k) \right|^2 \tag{82}$$

where

$\omega = 2\pi f$

$k = 2\pi\Omega$

The Fourier transforms were calculated in Part II. The constants f_o and Ω_o are chosen for normalization purposes and are related by $f_o = u\Omega_o$ corresponding to Equation 71. The value of f_o is taken from the measured duration of the time history $2T$ as $f_o = 1/(2T)$.

30. From Equations 76-82 it follows that the frequency response signatures can be written as

$$S_a(\omega) = \frac{u^2}{\omega^4}\left[\frac{I^a(\omega)}{I^h(k)}\right]^2 \tag{83}$$

$$S_v(\omega) = \frac{u^2}{\omega^2}\left[\frac{I^v(\omega)}{I^h(k)}\right]^2 \tag{84}$$

$$S_d(\omega) = u^2\left[\frac{I^d(\omega)}{I^h(k)}\right]^2 \tag{85}$$

where ω and k are releated by $\omega = uk$. Therefore the dimensionless frequency response signatures can be expressed in terms of the ratios of the Fourier transforms of the vehicle response to the Fourier transform of the obstacle profile.

31. The frequency response signatures can be rewritten in terms of transmission functions which are defined as follows

$$S_a(\omega) = T_a^2(\omega) \tag{86}$$

$$S_v(\omega) = T_v^2(\omega) \tag{87}$$

$$S_d(\omega) = T_d^2(\omega) \tag{88}$$

where

$T_a(\omega)$ = acceleration transmission function

$T_v(\omega)$ = velocity transmission function

$T_d(\omega)$ = displacement transmission function

which are found from Equations 83-85 to be

$$T_a(\omega) = \frac{u}{\omega^2} \frac{I^a(\omega)}{I^h(k)} \tag{89}$$

$$T_v(\omega) = \frac{u}{\omega} \frac{I^v(\omega)}{I^h(k)} \tag{90}$$

$$T_d(\omega) = \frac{uI^d(\omega)}{I^h(k)} \tag{91}$$

32. Because the dynamic response time histories of a point on a vehicle are very complex it is more convenient to use the Fourier series coefficients as calculated in Part II by the FFT rather than the Fourier transforms to calculate the frequency response signatures. The connection between the Fourier series coefficients and the Fourier transforms is given by Equation 69 and when this is combined with Equations 83-91 and $\omega_n = n\pi/T$ the following results are obtained

$$S_a(n) = \left(\frac{T}{n\pi}\right)^4 \left(\frac{C_n^a}{C_n^h}\right)^2 = T_a^2(n) \tag{92}$$

$$S_v(n) = \left(\frac{T}{n\pi}\right)^2 \left(\frac{C_n^v}{C_n^h}\right)^2 = T_v^2(n) \tag{93}$$

$$S_d(n) = \left(\frac{C_n^d}{C_n^h}\right)^2 = T_d^2(n) \tag{94}$$

where

$$T_a(n) = \left(\frac{T}{n\pi}\right)^2 \frac{C_n^a}{C_n^h} \tag{95}$$

$$T_v(n) = \frac{T}{n\pi} \frac{C_n^v}{C_n^h} \tag{96}$$

$$T_d(n) = \frac{C_n^d}{C_n^h} \tag{97}$$

for $n = 1, 2, 3, \ldots$. For $n = o$ the frequency response signatures are by definition equal to

$$S_a(o) = S_v(o) = S_d(o) = 1 \tag{98}$$

$$T_a(o) = T_v(o) = T_d(o) = 1 \tag{99}$$

Table 1 gives the dimensions of all the physical quantities that appear in this report.

33. From Equations 62-64 and $\omega_n = n\pi/T$ it follows that

$$T_a(n) = T_v(n) = T_d(n) = \frac{C_n^d}{C_n^h} \tag{100}$$

This follows from the assumption that the acceleration, velocity and displacement of a point on the vehicle can all be expanded as Fourier series with a common period $2T$ as shown in Equations 62-64.

34. Having obtained S_a, S_v and S_d from response data for a vehicle on a test obstacle, it is now possible to predict the RMS values of acceleration, velocity and displacement that are expected to occur at a point in the vehicle when it crosses another obstacle of known profile. This is done using Equations 73-75 where now the power spectrum $P_h(f) = P_h(\Omega)/u$ refers to the new obstacle. The new power spectrum is obtained using Equation 82 and the Fourier transform of the new obstacle profile. In this way the RMS dynamical response of a vehicle can be

predicted for any obstacle or any terrain elevation variation without having a specific dynamical model for the vehicle. Only the empirical frequency response signatures of a vehicle are required to predict the RMS dynamical response on any type of terrain. This is true only within the limits of the validity of the assumption that the acceleration, velocity, and displacement of a point on the vehicle can be written as Fourier series in the form given in Equations 62-64.

Model Description for the Frequency Response Signatures

35. In order to obtain a better understanding of the meaning of the frequency response signatures, their values for a simple vehicle-ground contact model is presented. Theoretical model-dependent expressions for the frequency spectrum signatures have already appeared in the literature and are as follows[8,9]:

$$S_a = |T_{dd}|^2 \, e^{-F}\begin{pmatrix} ASW^{(4)} & \text{wheels} \\ asw^{(4)} & \text{track} \end{pmatrix} \tag{101}$$

$$S_v = |T_{dd}|^2 \, e^{-F}\begin{pmatrix} ASW^{(2)} & \text{wheels} \\ asw^{(2)} & \text{track} \end{pmatrix} \tag{102}$$

$$S_d = |T_{dd}|^2 \, e^{-F} \quad \text{wheels or track} \tag{103}$$

where

$|T_{dd}|$ = magnitude of the displacement-displacement transmission function for vehicle

e^{-F} = low pass filter associated with the contact length of a wheel or track

$ASW^{(4)}$ = curvature spectral window function for wheeled vehicle

$asw^{(4)}$ = curvature spectral window function for track

$ASW^{(2)}$ = slope spectral window function for wheeled vehicle

$asw^{(2)}$ = slope spectral window function for track

36. Equations 101-103 show that in principle the frequency response signatures are independent of the obstacle profile and depend only on the geometric and dynamic characteristics of the vehicle. The dynamic characteristics enter through the displacement-displacement transmission function, while the geometry of the vehicle-obstacle contact area enters through the low pass filter associated with the spectral window functions and the low pass filter associated with the ground-vehicle contact length.[8,9] For a very small vehicle-ground contact length the frequency response spectra in Equations 101-103 reduce to the square of the dynamic transmission function.[8,9]

37. The contact length between the vehicle and the obstacle is very small (about 12 in.*) for the case of a vehicle crossing the small-sized obstacles that were used to obtain the experimental acceleration time histories treated in this report. This is true for both track and wheeled vehicles because the obstacles used for the tests are about 12 in. wide. For this case it follows from Equations 101-103 that

$$S_a = S_v = S_d = |T_{dd}|^2 \tag{104}$$

and the conditions for the validity of Equations 100 and 62-64 are satisfied. It follows that

$$T_a = |T_{dd}| \tag{105}$$

and the empirical values of the effective transmission function should be an accurate measure of the displacement-displacement transmission function for a vehicle.

Numerical Results

38. A numerical example of the theoretical procedures developed in this report will now be presented. The vertical acceleration time

---

* A table of factors for converting U. S. customary units of measurement to metric (SI) units is presented on page 3.

history at the drivers seat of an M114 track vehicle crossing a 6-in. radius semicircular obstacle at a speed $u = 5.2$ mph $= 91.5$ in./sec will be used to determine the transmission function from which the frequency response signature follows trivially as its square. The time history of the vertical acceleration at the drivers seat appears in Figure 6.

39. The Fourier series representation of the acceleration time history C_n^a was obtained from a measured period of $2T = 1.55$ sec using an FFT computer program and appears in Figure 7. The Fourier series representation of a 6-in. radius semicircular obstacle C_n^h was obtained for a period $2L = 2\mu T = 141.825$ in. using the analytical expression for the Fourier transform that appears in the table of transforms combined with Equation 39, and appears in Figure 8. The transmission function for the vehicle was then calculated using Equation 95 and the results appear in Figure 9.

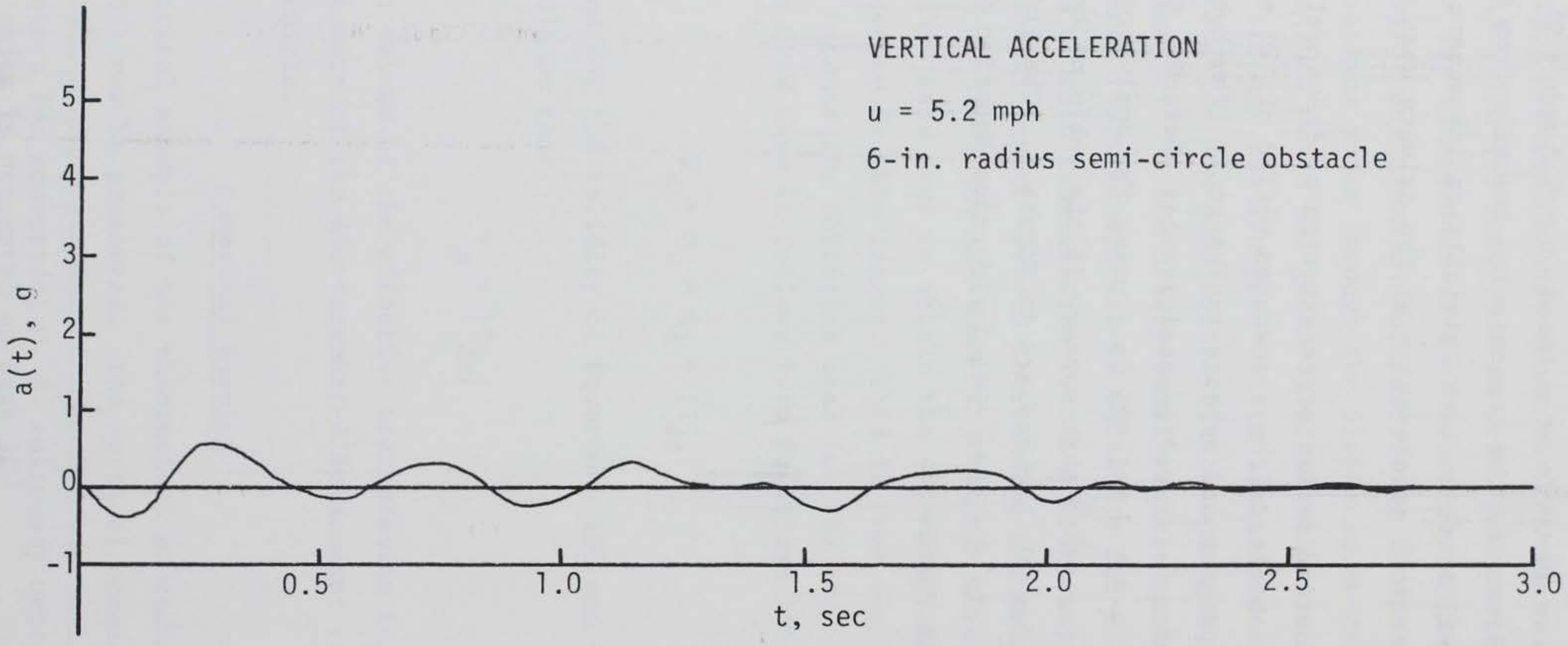

Figure 6. Acceleration time history for M114 track vehicle crossing a 6-in. semicircle obstacle at 5.2 mph

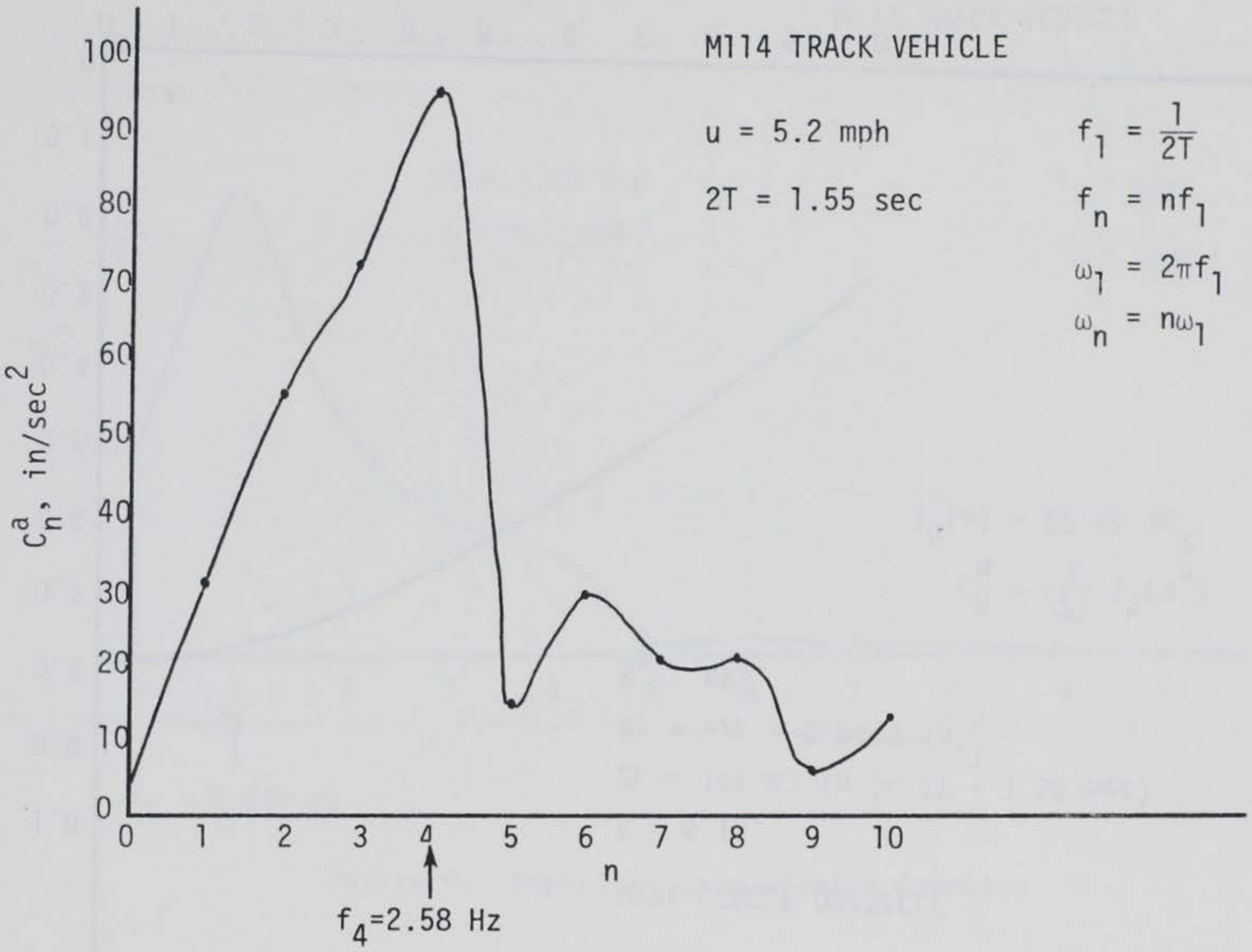

M114 TRACK VEHICLE

u = 5.2 mph

2T = 1.55 sec

$f_1 = \frac{1}{2T}$

$f_n = nf_1$

$\omega_1 = 2\pi f_1$

$\omega_n = n\omega_1$

Figure 7. Fourier series coefficients for acceleration

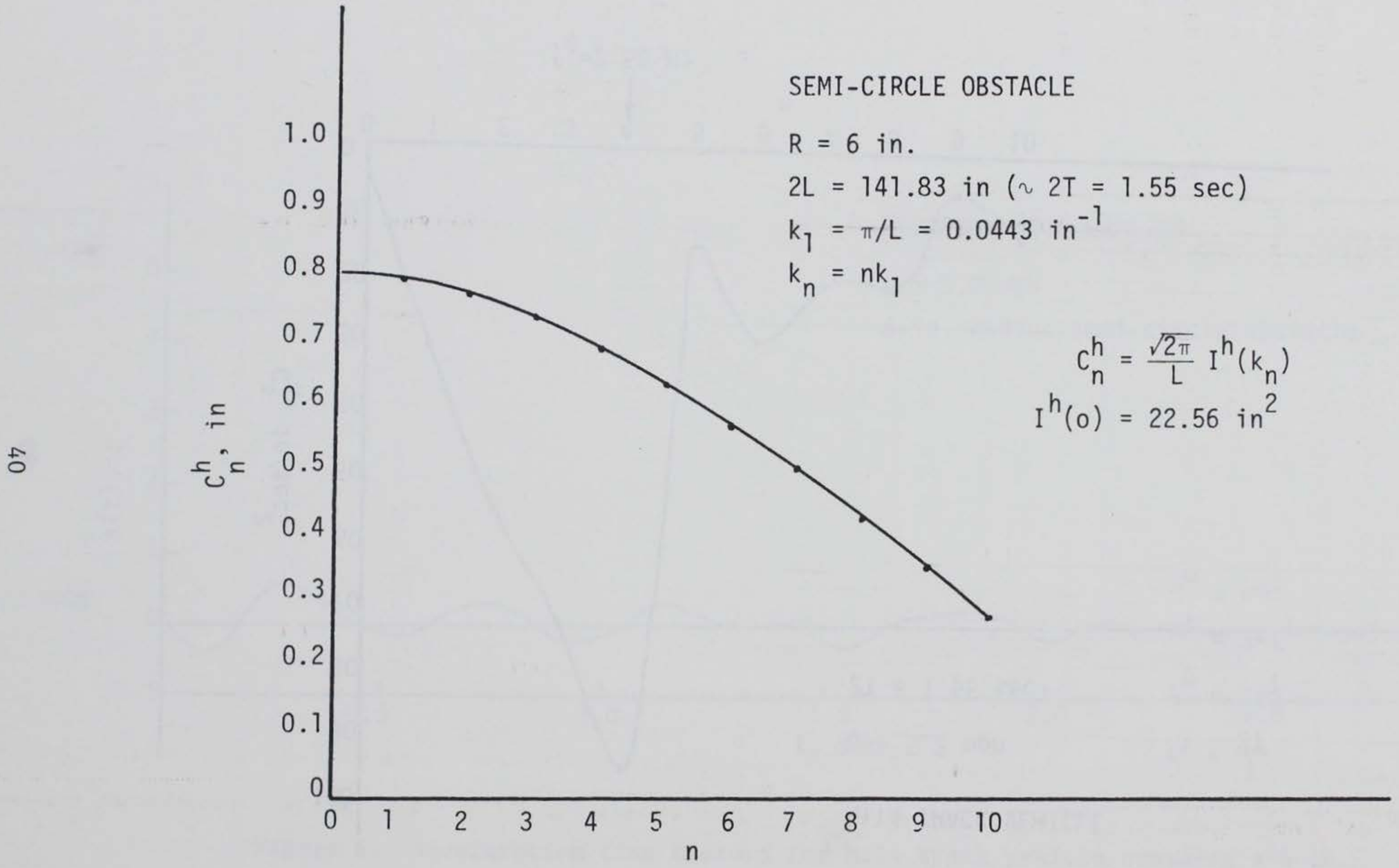

Figure 8. Fourier series coefficients for a 6-in. semicircular obstacle

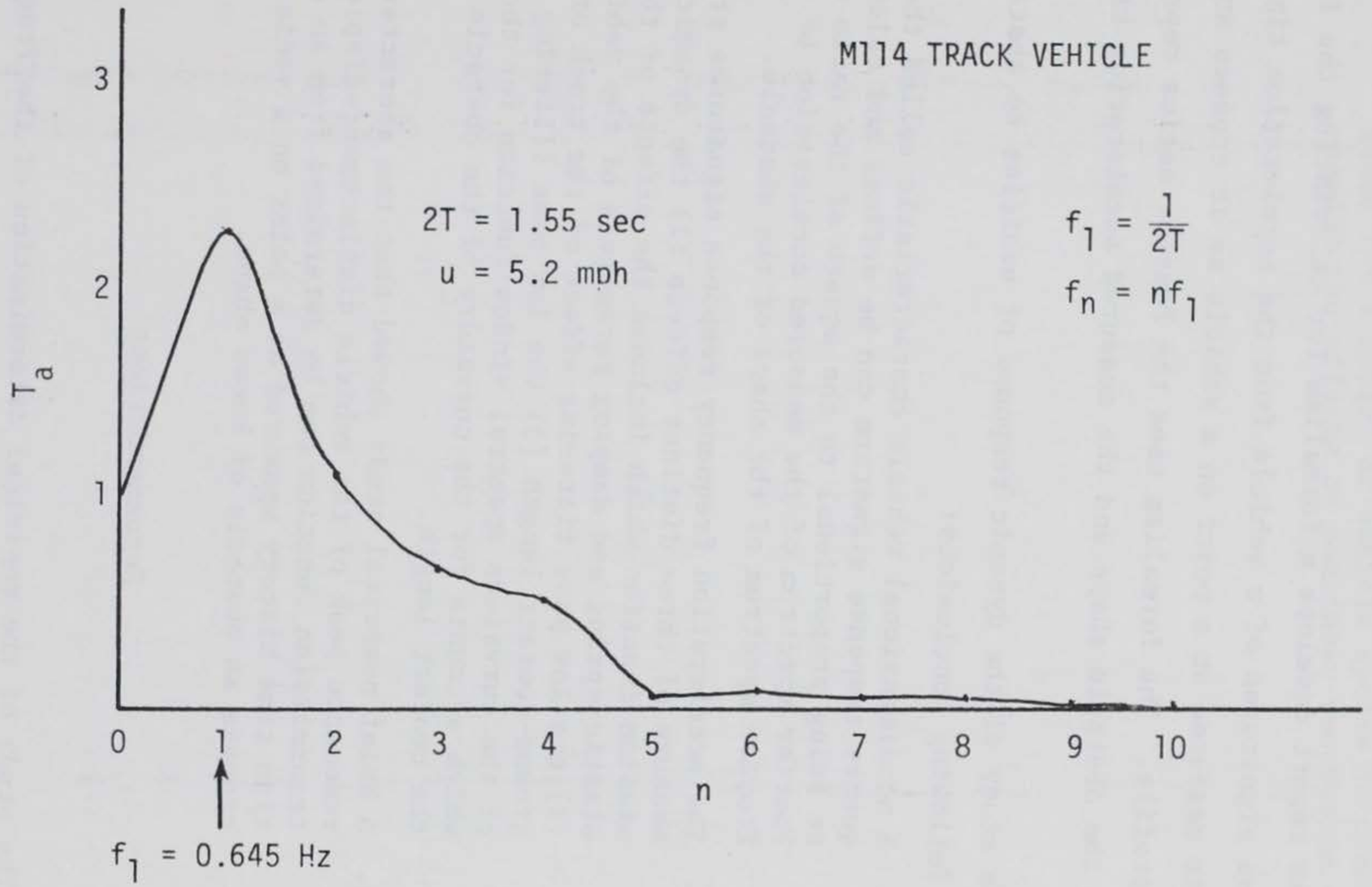

Figure 9. Empirical transmission function

PART IV: CONCLUSIONS AND RECOMMENDATIONS

Conclusions

40. This report develops a formalism for calculating the frequency response signatures of a vehicle from the acceleration time history that is measured at a point on a vehicle as it crosses an obstacle of known profile. The formalism uses the Fourier series representations of both the obstacle shape and the measured acceleration time history.

41. The study of the dynamic response of vehicles to obstacles produced the following conclusions:

a. A nondimensional vehicle characteristic called the frequency response signature can be defined and calculated as being proportional to the square of the ratio of the Fourier spectrum of the measured acceleration to the Fourier spectrum of the shape of the obstacle.

b. The acceleration frequency response signatures are a measure of three distinct effects (1) the dynamic transmission function which includes the effects of the mass, elastic spring and damping parameters of the vehicle (2) the low pass filtering effect of the track or wheel ground-contact length (3) the low pass filtering effect of the curvature spectral window function for the vehicle which accounts for the curvature of the obstacle over the contact length.

c. A brief numerical study showed that the characteristic resonance peak of the vehicle displacement-displacement transmission function can be determined from an acceleration time history measured at a point on a vehicle as it crosses an obstacle of known shape.

Recommendations

42. The study of the empirical determination of the frequency response signatures for vehicles produced several recommendations that will be helpful for the design of new vehicles. It is recommended that the following work be done:

a. Frequency response signatures should be determined

for a series of wheel and tracked vehicles and used to extract the effective damping and spring constants for these vehicles.

b. The frequency response signatures should be determined for a series of vehicle speeds in order to examine the effects of nonlinear suspension systems.

REFERENCES

1. Pradko, F., Lee, R. and Kaluza, V., "Theory of Human Vibration Response," presented at the Winter Annual Meeting and Energy Systems Exposition of the American Society of Mechanical Engineers, New York, N. Y., 27 Nov-1 Dec 1966.

2. Lins, W. F., "Human Vibration Response Measurement," Technical Report No. 11551, June 1972, U. S. Army Tank Automotive Command, Warren, Michigan.

3. Rocard, Y., General Dynamics of Vibration, Frederick Ungar Publishing Co., New York, 1960.

4. Bekker, M. G., "Introduction to Terrain-Vehicle Systems," University of Michigan Press, Ann Arbor, 1969.

5. Van Deusen, R. D., "A Statistical Technique for the Dynamic Analysis of Vehicles Traversing Rough Yielding and Non-yielding Surfaces," Contract Report No. NASW-1287, May 1966, Advanced Projects Organization, Chrysler Corp., Detroit, Mich.

6. Blackman, R. B. and Tukey, J. W., "The Measurement of Power Spectra," Dover Publications, New York, 1958.

7. Bendat, J. S. and Piersol, A. G., Random Data: Analysis and Measurement Procedures, Wiley-Interscience, New York, 1971.

8. Weiss, R. A., "Terrain Microroughness and the Dynamic Response of Vehicles," paper in 27th Conference of Army Mathematicians, West Point, New York, June 1981.

9. Weiss, R. A., "Characterization of Terrain Roughness, Vol I- Microroughness Description and its Applications to the Dynamic Response of Vehicles," Draft Report, U. S. Army Engineer Waterways Experiment Station, CE, Vicksburg, Miss.

10. Sneddon, I. N., Fourier Transforms, McGraw-Hill, New York, 1951.

11. Sneddon, I. N., Fourier Series, Routledge and Kegan Paul, London, 1961.

12. Emerson, P. L., "Fast Fourier Transform Fundamentals and Applications," Creative Computing, pgs. 58-63, July 1980.

13. Liu, B., editor, Digital Filters and the Fast Fourier Transform, Halsted Press, Stroudsburg, Pa.

Table 1

Dimensions of Physical Quantities

Physical Quantity	Units
Obstacle profile height $h(x)$	in.
Displacement at a point on vehicle $d(t)$	in.
Velocity at a point on vehicle $v(t)$	in./sec
Acceleration at a point on vehicle $a(t)$	$in./sec^2$
Fourier transform of obstacle profile $I^h(k)$	$in.^2$
Fourier transform of displacement $I^d(f)$	in. sec
Fourier transform of velocity $I^v(f)$	in.
Fourier transform of acceleration $I^a(f)$	in./sec
Fourier coefficients of obstacle profile C_n^h	in.
Fourier coefficients of displacement C_n^d	in.
Fourier coefficients of velocity C_n^v	in./sec
Fourier coefficients of acceleration C_n^a	$in./sec^2$
Power spectrum of obstacle profile $P_h(\Omega)$	$in.^3$
Power spectrum of displacement $P_d(f)$	$in.^2$ sec
Power spectrum of velocity $P_v(f)$	$in.^2/sec$
Power spectrum of acceleration $P_a(f)$	$in.^2/sec^3$
Time period of acceleration $2T$	sec
Space period of obstacle $2L = 2uT$	in.
Obstacle length $2L_o$	in.

APPENDIX A: CALCULATION OF FOURIER TRANSFORMS OF OBSTACLE SHAPES

1. This appendix gives a sketch of the calculations used to determine the Fourier transforms of the basic obstacle shapes considered in this report. The problem is to calculate the Fourier cosine and sine transforms defined as

$$I_c^h = \frac{1}{\sqrt{2\pi}} \int_{-\infty}^{\infty} h(x) \cos kx dx \tag{A1}$$

$$I_s^h = \frac{1}{\sqrt{2\pi}} \int_{-\infty}^{\infty} h(x) \sin kx dx \tag{A2}$$

where $h(x)$ equals the height profile of the obstacle. The vehicle is assumed to be moving from left to right, so that the left edge of the obstacle is encountered first and it is at this point that the acceleration response time history of the vehicle begins. Therefore the origin of the axis is placed at the left edge of the obstacle. For an obstacle of length $2L_o$ the integrals in Equations A1 and A2 can be written as

$$I_c^h = \frac{1}{\sqrt{2\pi}} \int_{o}^{2L_o} h(x) \cos kx dx \tag{A3}$$

$$I_s^h = \frac{1}{\sqrt{2\pi}} \int_{o}^{2L_o} h(x) \sin kx dx \tag{A4}$$

where x equals the coordinate measured from the left edge of the obstacle.

2. It is helpful to introduce the following coordinate transformation

$$x = L_o + \xi \tag{A5}$$

Then the integrals in Equations A3 and A4 can be written as

$$I_c^h = \frac{1}{\sqrt{2\pi}} \int_{-L_o}^{L_o} h(\xi)(\cos kL_o \cos k\xi - \sin kL_o \sin k\xi)d\xi \tag{A6}$$

$$I_s^h = \frac{1}{\sqrt{2\pi}} \int_{-L_o}^{L_o} h(\xi)(\sin kL_o \cos k\xi + \cos kL_o \sin k\xi)d\xi \tag{A7}$$

If the obstacle is symmetrical the sine integrals in Equations A6 and A7 vanish and the cosine integrals are symmetric so that

$$I_c^h = \cos kL_o \sqrt{\frac{2}{\pi}} \int_o^{L_o} h(\xi) \cos k\xi d\xi \tag{A8}$$

$$I_s^h = \sin kL_o \sqrt{\frac{2}{\pi}} \int_o^{L_o} h(\xi) \cos k\xi d\xi \tag{A9}$$

which can be rewritten as

$$I_c^h = F_c^h \cos kL_o \tag{A10}$$

$$I_s^h = F_c^h \sin kL_o \tag{A11}$$

where F_c^h is the Fourier cosine transform defined as

$$F_c^h = \sqrt{\frac{2}{\pi}} \int_o^{L_o} h(\xi) \cos k\xi d\xi \qquad \text{(A12)}$$

Therefore for symmetrical obstacles it is only necessary to calculate the Fourier cosine tranform F_c^h because I_c^h and I_s^h follow automatically from Equations A10 and A11. For asymmetrical obstacles both I_c^h and I_s^h must be calculated separately.

3. The following parts of this appendix gives the evaluation of the Fourier transforms of some basic obstacle shapes. Symmetrical obstacles are treated first and then their asymmetrical counterparts are considered.

Symmetrical Obstacles

Semicircular obstacle (Figure 4a)

4. The semicircle is described by $L_o = R$ and

$$h(\xi) = R\sqrt{1 - \xi^2/R^2} \qquad \text{(A13)}$$

for $|\xi| \leq R$, where ξ is measured from the symmetry axis. The function is symmetrical and the Fourier cosine transform is given as

$$F_c^h(k) = \sqrt{\frac{2}{\pi}} \int_o^R R\sqrt{1 - \xi^2/R^2} \cos k\xi d\xi \qquad \text{(A14)}$$

The substitution $\eta = \xi/R$ gives

$$F_c^h(k) = \sqrt{\frac{2}{\pi}} R^2 \int_o^1 \sqrt{1 - \eta^2} \cos (kR\eta) d\eta \qquad \text{(A15)}$$

But from the table in Sneddon's book[10] it follows that

$$\sqrt{\frac{2}{\pi}}\int_0^1 \sqrt{1-\eta^2}\,\cos\,(kR\eta)d\eta = \sqrt{\frac{\pi}{2}}\,\frac{J_1(kR)}{kR} \tag{A16}$$

where $J_1(kR)$ equals the first order Bessel function. Then it follows that the Fourier transform of the semicircle is

$$F_c^h(k) = R^2\sqrt{\frac{\pi}{2}}\,\frac{J_1(kR)}{kR} \tag{A17}$$

$$= \sqrt{\frac{2}{\pi}}\left(\frac{\pi}{4}R^2\right)\left[\frac{2J_1(kR)}{kR}\right]$$

For small kR one has $J_1(kR) \sim kR/2$, so that

$$F_c^h(k) \to \frac{1}{2}\sqrt{\frac{\pi}{2}}\,R^2 = 0.62666R^2 \tag{A18}$$

For large kR

$$J_1(kR) \sim \sqrt{\frac{2}{\pi kR}}\,\cos\,(kR - 3\pi/2) \tag{A19}$$

and the Fourier transform is obtained from Equation A17 to be

$$F_c^h(k) \to \sqrt{\frac{\pi}{2}}\,\frac{R}{k}\,\sqrt{\frac{2}{\pi kR}}\,\cos\,(kR - 3\pi/2) \tag{A20}$$

The zeros of $J_1(kR)$ are given in the references and are determined by

$$J_1(k_nR) = 0 \tag{A21}$$

which gives

$$k_nR = r_n \tag{A22}$$

where r_n equals the n'th root of the first order Bessel function. The roots of J_1 are tabulated in the literature and the first few are as follows

$$r_1 = 3.8317 \tag{A23}$$

$$r_2 = 7.0156 \tag{A24}$$

$$r_3 = 10.1735 \tag{A25}$$

Therefore the values of k, Ω, and λ for the roots are

$$k_n = \frac{r_n}{R} \tag{A26}$$

$$\Omega_n = \frac{r_n}{2\pi R} \tag{A27}$$

$$\lambda_n = \frac{2\pi R}{r_n} \tag{A28}$$

Rectangular obstacle (Figure 4b)

5. The rectangle is described by $h(\xi) = h$ for $0 < \xi < a$ where ξ is measured from the axis as symmetry, and the Fourier cosine transform for this symmetrical obstacle with $L_o = a$ is

$$F_c^h(k) = \sqrt{\frac{2}{\pi}} \int_o^a h \cos k\xi d\xi$$

$$= h \sqrt{\frac{2}{\pi}} \frac{\sin (ka)}{k} \tag{A29}$$

$$= \sqrt{\frac{2}{\pi}} (ah) \left[\frac{\sin (ka)}{ka} \right]$$

The zeros occur at

$$k_n a = n\pi \tag{A30}$$

The values of k, Ω, and λ at the roots are

$$k_n = \frac{n\pi}{a} \tag{A31}$$

or

$$\Omega_n = \frac{n}{2a} \tag{A32}$$

$$\lambda_n = \frac{2a}{n} \tag{A33}$$

Symmetrical trapezoid (Figure 4c)

6. The symmetrical trapezoid is described by the following functions with the origin of coordinates chosen at the axis of symmetry and $L_o = a + b$

$$h(\xi) = \begin{cases} h & 0 < \xi < a \\ \frac{h}{b}(a + b - \xi) & a < \xi < a + b \end{cases} \tag{A34}$$

where the coordinate ξ is measured from the symmetry axis. The Fourier cosine transform is given by

$$F_c^h(k) = \sqrt{\frac{2}{\pi}} \int_o^a h \cos k\xi d\xi + \sqrt{\frac{2}{\pi}} \int_a^{a+b} \frac{h}{b}(a + b - \xi) \cos k\xi d\xi$$

$$= \sqrt{\frac{2}{\pi}} \frac{h}{bk^2} [\cos ka - \cos k(a + b)] \tag{A35}$$

$$= \sqrt{\frac{2}{\pi}} \left(a + \frac{b}{2}\right) h \left[\frac{\sin k(a + b/2)}{k(a + b/2)}\right] \left[\frac{\sin (kb/2)}{kb/2}\right]$$

The limit $b \to 0$ reproduces the results for the rectangle shown in case 2.

Symmetrical triangle (Figure 4d)

7. The case of the symmetrical triangle can be obtained from the symmetrical trapezoid by taking $a = 0$. From the result in case 3 for the symmetrical trapezoid it follows that the symmetrical triangle is obtained with $a = 0$ to be

$$F_c^h(k) = \sqrt{\frac{2}{\pi}} \left(\frac{bh}{2}\right)\left[\frac{\sin\ (kb/2)}{kb/2}\right]^2 \tag{A36}$$

and the obstacle half-length is $L_o = b$.

Double rectangle (Figure 4e)

8. The double rectangle obstacle can be represented as follows

$$h(\xi) = \begin{cases} h_1 & 0 < \xi < a \\ h_2 & a < \xi < a + c \end{cases} \tag{A37}$$

where

ξ = coordinate measured from the symmetry axis

$L_o = a + c$

The Fourier cosine transform is

$$F_c^h(k) = \sqrt{\frac{2}{\pi}} \int_o^a h_1 \cos k\xi d\xi + \sqrt{\frac{2}{\pi}} \int_a^{a+c} h_2 \cos k\xi d\xi$$

$$= \sqrt{\frac{2}{\pi}} \left\{ h_1 \frac{\sin ka}{k} + h_2 \left[\frac{\sin k(a + c)}{k} - \frac{\sin ka}{k}\right]\right\} \tag{A38}$$

$$= \sqrt{\frac{2}{\pi}} \left[h_1 a \frac{\sin ka}{ka} + h_2 c \frac{\sin kc/2}{kc/2} \cos k(a + c/2)\right]$$

For $c = 0$ this reduces to case 2 of the rectangle of height h_1 , while for $a = 0$ it reduces to case 2 of the rectangle of height h_2 .

Asymmetrical Obstacles

Asymmetrical trapezoid (Figure 5a)

9. The origin of the axis is taken at the left edge of the obstacle whose total length is $2L_o = 2a + b + e$. The equations defining the shape of the obstacle are

$$h(x) = \begin{cases} \frac{h}{b}\, x & a < x < b \\ h & b < x < 2a + b \\ \frac{h}{e}\,(2a + b + e - x) & 2a + b < x < 2a + b + e \end{cases} \qquad \text{(A39)}$$

The cosine component of the Fourier transform is

$$I_c^h = \frac{1}{\sqrt{2\pi}} \int_o^b \frac{h}{b}\, x \cos kx + \frac{1}{\sqrt{2\pi}} \int_b^{2a+b} h \cos kx dx \qquad \text{(A40)}$$

$$+ \frac{1}{\sqrt{2\pi}} \int_{2a+b}^{2a+b+e} \frac{h}{e}\,(2a + b + e - x) \cos kx dx$$

After some algebra the cosine component is found to be

$$I_c^h = \frac{1}{\sqrt{2\pi}} \frac{h}{k} \left[\sin k\left(2a + b + \frac{e}{2}\right)\left(\frac{\sin ke/2}{ke/2}\right) - \frac{kb}{2}\left(\frac{\sin kb/2}{kb/2}\right)^2 \right] \qquad \text{(A41)}$$

The sine component of the Fourier transform is given by

$$I_s^h = \frac{1}{\sqrt{2\pi}} \int_o^b \frac{h}{b}\, x \sin kx dx + \frac{1}{\sqrt{2\pi}} \int_b^{2a+b} h \sin kx dx \qquad \text{(A42)}$$

$$+ \frac{1}{\sqrt{2\pi}} \int_{2a+b}^{2a+b+e} \frac{h}{e}\,(2a + b + e - x) \sin kx dx$$

Some algebra gives the sine component of the Fourier transform as

$$I_s^h = \frac{1}{\sqrt{2\pi}} \frac{h}{k} \left[\frac{\sin kb}{kb} - \left(\frac{\sin ke/2}{ke/2} \right) \cos k\left(2a + b + \frac{e}{2}\right) \right] \qquad \text{(A43)}$$

The magnitude of the Fourier transform is then obtained as

$$I^h = \sqrt{\left(I_c^h\right)^2 + \left(I_s^h\right)^2} \qquad \text{(A44)}$$

$$= \frac{1}{\sqrt{2\pi}} \frac{h}{k} \sqrt{\left(\frac{\sin kb/2}{kb/2}\right)^2 + \left(\frac{\sin ke/2}{ke/2}\right)^2 - 2\left(\frac{\sin kb/2}{kb/2}\right)\left(\frac{\sin ke/2}{ke/2}\right) \cos k\left[2a + \frac{(b + e)}{2}\right]}$$

Note Equation A44 is symmetric under interchange of the variables b and e .

Right angle trapezoid (Figure 5b)

10. The right angle trapezoid can be obtained as a special case of the general asymmetrical trapezoid by taking e = 0 in case 1. The results are

$$I_c^h = \frac{1}{\sqrt{2\pi}} \frac{h}{k} \left[\sin k(2a + b) - \frac{kb}{2} \left(\frac{\sin kb/2}{kb/2} \right)^2 \right] \qquad \text{(A45)}$$

$$I_s^h = \frac{1}{\sqrt{2\pi}} \frac{h}{k} \left[\frac{\sin kb}{kb} - \cos k(2a + b) \right] \qquad \text{(A46)}$$

$$I^h = \frac{1}{\sqrt{2\pi}} \frac{h}{k} \sqrt{1 + \left(\frac{\sin kb/2}{kb/2}\right)^2 - 2\left(\frac{\sin kb/2}{kb/2}\right) \cos k\left(2a + \frac{b}{2}\right)} \qquad \text{(A47)}$$

Asymmetrical triangle (Figure 5c)

11. The asymmetrical triangle can be obtained as a special case of the general asymmetrical trapezoid by taking a = 0 in the results of case 1. The results are

$$I_c^h = \frac{h}{\sqrt{2\pi k}} \left[\sin k\left(b + \frac{e}{2}\right)\left(\frac{\sin ke/2}{ke/2}\right) - \frac{kb}{2}\left(\frac{\sin kb/2}{kb/2}\right)^2 \right] \tag{A48}$$

$$I_s^{h'} = \frac{h}{\sqrt{2\pi k}} \left[\frac{\sin kb}{kb} - \left(\frac{\sin ke/2}{ke/2}\right) \cos k\left(b + \frac{e}{2}\right) \right] \tag{A49}$$

$$I^h = \frac{h}{\sqrt{2\pi k}} \sqrt{\left(\frac{\sin kb/2}{kb/2}\right)^2 + \left(\frac{\sin ke/2}{ke/2}\right)^2 - 2\left(\frac{\sin kb/2}{kb/2}\right)\left(\frac{\sin ke/2}{ke/2}\right) \cos k\left(\frac{b+e}{2}\right)} \tag{A50}$$

Right triangle (Figure 5d)

12. The Fourier transform of the right triangle can be obtained as a special case of the asymmetrical triangle (case 3) by taking either $b = 0$ or $e = 0$ depending on whether the right angle faces the moving vehicle or not.

a. Right angle facing vehicle ($b = 0$)

$$I_c^h = \frac{h}{\sqrt{2\pi k}} \left(\frac{ke}{2}\right)\left(\frac{\sin ke/2}{ke/2}\right)^2 \tag{A51}$$

$$I_s^h = \frac{h}{\sqrt{2\pi k}} \left(1 - \frac{\sin ke}{ke}\right) \tag{A52}$$

$$I^h = \frac{h}{\sqrt{2\pi k}} \sqrt{1 + \left(\frac{\sin ke/2}{ke/2}\right)^2 - 2\,\frac{\sin ke}{ke}} \tag{A53}$$

b. Right angle facing away from vehicle ($e = 0$)

$$I_c^h = \frac{h}{\sqrt{2\pi k}} \left[\sin kb - \frac{kb}{2}\left(\frac{\sin kb/2}{kb/2}\right)^2 \right] \tag{A54}$$

$$I_s^h = \frac{h}{\sqrt{2\pi k}} \left(\frac{\sin kb}{kb} - \cos kb\right) \tag{A55}$$

$$I^h = \frac{h}{\sqrt{2\pi k}} \sqrt{1 + \left(\frac{\sin kb/2}{kb/2}\right)^2 - 2\,\frac{\sin kb}{kb}} \qquad \text{(A56)}$$